

promoting access to White Rose research papers



Universities of Leeds, Sheffield and York
<http://eprints.whiterose.ac.uk/>

This is an author produced version of a paper published in **Tribology International**.

White Rose Research Online URL for this paper:
<http://eprints.whiterose.ac.uk/43104/>

In Press Paper

Kasolang, S., Ahmad, M.A. and Dwyer-Joyce, R.S. (2011) *Measurement of circumferential viscosity profile in stationary journal bearing by shear ultrasonic reflection*. Tribology International. (In Press).

<http://dx.doi.org/10.1016/j.triboint.2011.04.014>

Measurement of Circumferential Viscosity Profile in Stationary Journal Bearing by Shear Ultrasonic Reflection

S.Kasolang , M.A. Ahmad
 Faculty of Mechanical Engineering
 Universiti Teknologi MARA
 Malaysia
 salmiah99@hotmail.com, alie_76_02@yahoo.com

R.S. Dwyer Joyce
 Department of Mechanical Engineering
 University of Sheffield
 Sheffield, UK
 r.dwyerjoyce@shffield.ac.uk

Abstract— Viscosity is the most important lubricant property that affects bearing performance. It controls the film thickness that is established during operation. In this study, an ultrasonic method was used to measure the viscosity profile around a static journal bearing by using shear reflection coefficients. The technique introduced was found to be promising and acceptable results were obtained for certain regions of the journal bearing circumference. It proved to be critical to use the right model for determining viscosity from the layer response to a shear ultrasonic pulse. This study serves as a preliminary work for developing viscosity measurement in a rotating journal bearing.

Keywords - Viscosity profile; Ultrasound Shear-Wave; Reflection Coefficient; Journal Bearing; Transducer;

I. INTRODUCTION

Fluid viscosity in bulk is readily measured by using different types of viscometer on captive of flowing oil samples. However, inside a journal bearing where the lubricant exists in a thin layer, the use of viscometer is not feasible; hence an alternative means is required. The use of an ultrasonic approach to measure viscosity in bulk fluid has been reported [1, 2] but the approach has not previously been extended to measure the viscosity in the thin films fluid that exist in machine elements.

Earlier work that measures viscosity in thin layers between parallel plates by using shear reflection coefficient [3, 4] concluded that the phase method was more appropriate for thinner layers with lower Sommerfeld numbers. This method has been validated and an agreement was achieved via independent means of measurement.

In this study, an ultrasonic means was used to measure shear reflection coefficients at different locations around a journal bearing in static conditions (i.e. applied load, but no velocity and hence no circumferential temperature change and constant viscosity). The reflection coefficient data were then converted to viscosity values and compared against the predicted values using both a *bulk model* and an *interfacial spring model* approach.

These two models have been evaluated thick and thin fluid layers respectively. Judgment on the layer thickness can be approximated by the ultrasonic wavelength.

II. LITERATURE REVIEW

A. Correlating Reflection Coefficient to Viscosity with a Bulk Model

The acoustic impedance of the fluid medium [5], can be expressed as a complex number as follows,

$$z_{liq} = \left(\frac{\omega \rho \eta}{2} \right)^{0.5} (1+i) \quad (1)$$

Equation (1) expresses the acoustic impedance of the fluid in terms of the frequency of the propagating shear wave, fluid density and fluid viscosity.

The acoustic impedance may be expressed as a function of reflection coefficient of the shear wave as discussed [1]. If the acoustic impedance of the liquid and solid are known, the reflection coefficient R can be computed [1, 6]. The equation can be simplified as,

$$z_{liq} = z_s \frac{(1-R)^2}{(1+R)^2} + iz_s \frac{(2R \sin \theta)}{(1+R)^2} \quad (2)$$

Equation (2) expresses the acoustic impedance of the fluid as a function of the acoustic impedance of a solid and the reflection of a shear wave. Equating the real part of both equations produces a mathematical relation that relates fluid viscosity and the reflection coefficient. This relation can be arranged to give the density-viscosity product so that,

$$(\rho \eta)^{0.5} = \rho_s c_s \left(\frac{2}{\omega} \right)^{0.5} \left(\frac{1-R}{1+R} \right) \quad (3)$$

Alternatively, (3) can be rearranged to give the reflection coefficient, R as:-

$$R = \frac{1-X}{1+X}; \quad X = \frac{(\rho \eta)^{0.5}}{\rho_s c_s \left(\frac{2}{\omega} \right)^{0.5}} \quad (4)$$

where ρ_s and c_s are the density-viscosity product in the solid (load material). The viscosity of the fluid may be computed from the measurement of the reflection coefficient if other properties of (3) are known. Equation (4) is shown graphically in Fig. 1 for the reflection from a Perspex-oil interface (acoustic properties given in table 1).

It is clear that the reflection coefficient spectra for shear waves have a negative slope, indicating that the reflection coefficient decreases with increasing frequency. It is also noted that at low viscosity the reflection coefficient is larger.

Table 1 Acoustic properties of several materials (Krautkramer and Krautkramer, 1990)

Material	Density (kg/m ³)	Shear Velocity (m/s)
Perspex	1180	1430
Oil	884	31
Brass	8560	2300

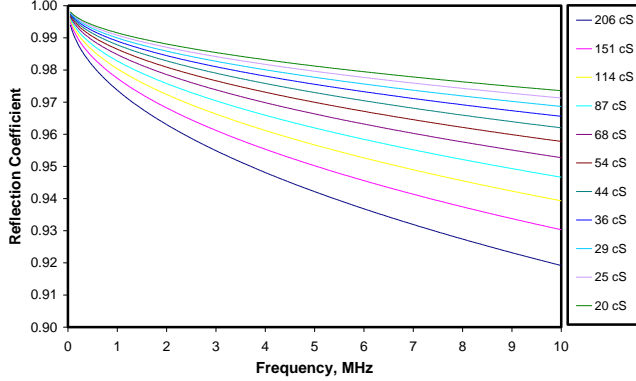


Figure 1 Predicted shear reflection coefficient from Perspex-oil interface at different viscosity values (equation 4).

B. Correlating Reflection Coefficient to Viscosity with a Spring Model

Fig. 2 schematically shows a thin layer of liquid trapped between two solid bodies. The layer is so thin, compared with the ultrasonic wavelength, that it essentially acts as a single reflector and in the proportion of the wave reflected depends on the stiffness of the layer [4,7,8]. The mathematical expression that relates reflection coefficient, R to K is given as,

$$R = \frac{(z_1 - z_2) + \frac{i\omega}{K}(z_1 z_2 - z_0^2)}{(z_1 + z_2) + \frac{i\omega}{K}(z_1 z_2 + z_0^2)} \quad (5)$$

where z defined as acoustic impedance of the media and subscript 0 refers to the layer, and 1 and 2 refer to either side of the layer.

The reflection coefficient from (5) is a complex quantity containing both amplitude and phase information. It can be applied to both longitudinal and shear waves. For a longitudinal wave, the longitudinal velocity and the longitudinal interfacial stiffness must be used. In the case of shear wave, the shear velocity and the shear interfacial stiffness are appropriate. For a thin viscous liquid layer, the interfacial shear stiffness K is given by [9] as,

$$K = \frac{i\omega\eta}{h} \quad (6)$$

By putting (6) into (5), it gives,

$$R = \frac{(z_1 - z_2) + \frac{h}{\eta}(z_1 z_2 - z_0^2)}{(z_1 + z_2) + \frac{h}{\eta}(z_1 z_2 + z_0^2)} \quad (7)$$

Further simplified for similar materials on either side of the fluid layer $z_1 = z_2 = z_s$ (acoustic impedance of solid), (7) can be rewritten as,

$$R = \frac{\frac{h}{\eta}(z_s^2 - z_o^2)}{2z_s + \frac{h}{\eta}(z_s^2 - z_o^2)} \quad (8)$$

Rearranging (8) to give the ratio of viscosity over thickness, it becomes,

$$\frac{\eta}{h} = \frac{(z_s^2 - z_o^2)(R-1)}{-2Rz_s} \quad (9)$$

The equation shows the correlation between viscosity and reflection coefficient. In Fig. 3, equation (7) is plotted for various combinations of materials on either side of the oil film. The reflection coefficient amplitude is plotted as a function of the viscosity-thickness ratio for each combination.

Unlike the bulk model, the spring model is dependent on the film thickness and hence there should be one predicted thickness spectrum for every experimental thickness spectrum. The thickness where the spring model remains valid can also be approximated, which is 25.8 micron in this study.

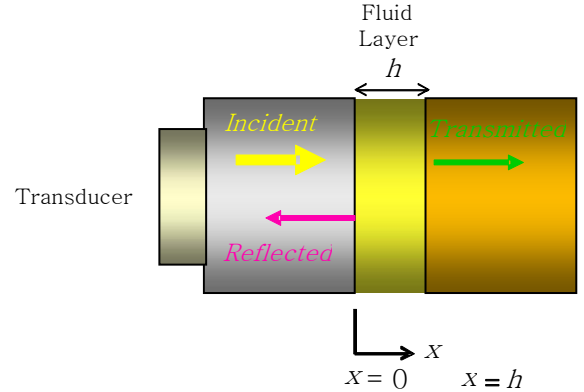


Figure 2 Schematic diagram of an ultrasonic wave reflected at a thin layer

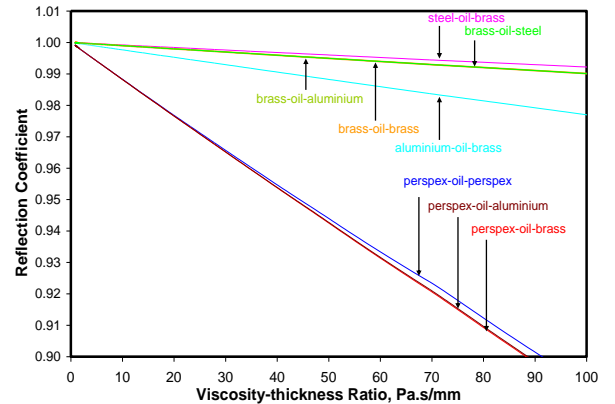


Figure 3 Predicted reflection coefficient of an ultrasonic shear wave from an oil layer between different materials

III. APPARATUS

A. Ultrasonic signal processing equipment

The ultrasonic equipment used in this study is shown in Fig. 4. The main components are a computer, an ultrasonic pulser receiver (UPR), a digitizer (oscilloscope), and a transducer. The UPR generates short duration voltage pulses which excite the transducer causing it to resonate, thus sending the required ultrasonic pulse to the medium.

The transducer operates in a pulse-echo mode. The transducer converts electrical signals supplied by UPR into a mechanical vibration. When the pulse encounters the boundary, it is partially reflected and received by the same transducer. The reflected pulse is converted to a voltage by the transducer, amplified by the UPR, digitized by the oscilloscope and then passed through the computer for processing. A series of LabView routines control the operation of the hardware and the subsequent processing of the received signals.

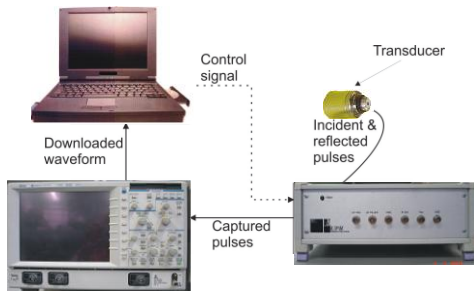


Figure 4 Schematic diagrams of ultrasonic measurement apparatus

B. Plug Design and Transducer installation

A plug was needed for the test material onto which the PZT element was bonded. The plug was made from a Perspex cylinder of length and diameter 10mm.

The shear ultrasonic transducer used was a rectangular piezoelectric element with 1-mm thickness, 7-mm length and 5-mm width. The centre frequency was 1.2 MHz. The PZT element that was attached to a plug (Fig. 5) was then fixed into a journal. The wires were then fed back through slip rings to the pulsing-receiving circuit. The PZT element and the soldered contacts were then covered in a protective layer of epoxy to secure the delicate contacts during assembly and testing.

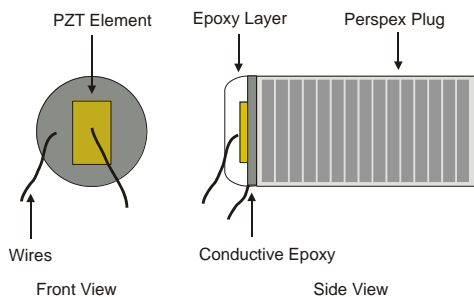


Figure 5 Schematic of piezo-electric transducer and plug

C. Modification of Journal Bearing Test Apparatus

The journal test rig was modified by preparing a hole on the journal and the shear transducer assembly was then fixed by pressing it into the hole (Fig. 6). The protruding part of the Perspex plug was machined in order to follow the contour of the journal. The journal bearing was then measured and the new clearance determined.

Oil temperature was recorded using thermocouples at the oil supply hole and at the outlet of the bearing. Bearing load and speed were then monitored throughout by using a simple load cell and laser tachometer.

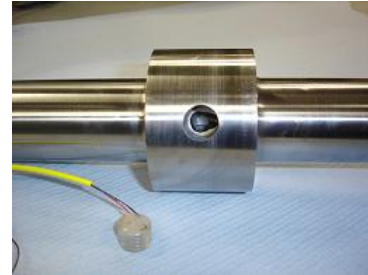


Figure 6 A shear transducer ready to be placed into the shaft

D. Journal Bearing Circumference

The circumference around the journal bearing is classified as shown in Fig. 7. The spring model is expected to give good approximation where the oil film is thin (the lower portion from 127° to 233° as shown). Anti-clockwise notion of the bearing angle was used due to the direction of the journal bearing rotation.

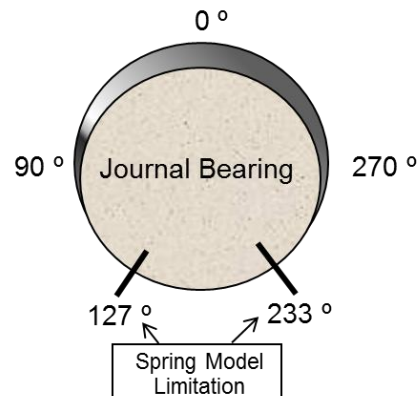


Figure 7 Regions around the stationary journal were defined.

IV. RESULTS

A. Reflection Coefficient Profile

The recorded shear reflection coefficient profiles obtained around the circumference of the journal are shown in Fig. 8. The reflection coefficient spectra from each region as defined in Fig. 7 were separated by the inclination of the spectra. The spectra from the thin film region were flatter than the spectra from the thick film region. This means that the spectra in the thin film region were less

affected by the frequency; notice how equation (3) is frequency dependent but equation (9) is not. The spectra for the 90^0 and 270^0 degrees region turned out to be slightly different. This is because the bearing bush does not follow an exact circular profile.

Earlier studies [4, 10], show that the bulk model worked better in thick films and the spring model in thin films. The bulk model is applied to the data acquired from 0^0 to 120^0 and 240^0 to 330^0 regions and the Spring Model to the data acquired from 120^0 to 240^0 region.

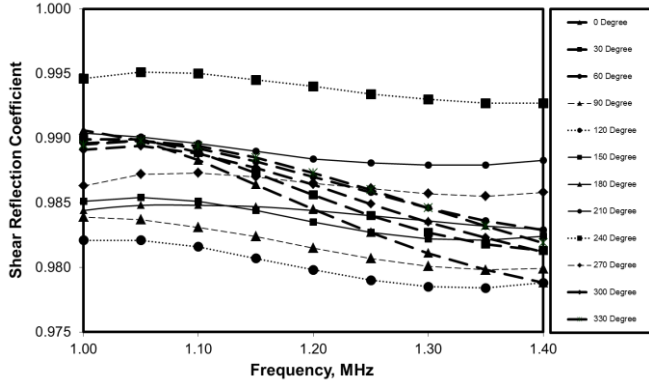


Figure 8 Reflection coefficient profile around journal bearing

B. Application of Bulk Model to Thick Films and Spring Model to Thin Films

The experimental reflection coefficient spectra from the thick films are plotted as Fig. 9. The predicted reflection coefficient spectra obtained by using the bulk model from equation (3) is also shown for the case when the temperature is 20°C and the viscosity determined from the datasheet. The reflection coefficient is expected to be independent of thickness and should give the same viscosity value as the corresponding viscosity determined from the lubricant data sheet. From Fig. 7 it can be seen that the experimental reflection coefficient in the 0^0 to 90^0 and 270^0 to 360^0 regions was actually less affected by the variation in the film thickness and hence, consistent with the bulk model.

The experimental reflection coefficient spectra at 180^0 , 210^0 and 240^0 degrees were re-plotted as Fig. 10. The predicted reflection coefficient spectra were obtained by using the spring model equation (9). The spring model is dependent on the film thickness and so there is not one unique curve. From Fig. 10, it can be seen that the experimental reflection coefficient spectra agree well with the predicted spectra. The eccentricity ratio was computed and the thickness profile was generated as shown in Fig. 11 by assuming that the bearing is smooth and lacks form error.

If the thickness in the 120^0 and 150^0 regions is same as 210^0 and 240^0 regions, a similar observation as Fig. 10 should be expected. However, the results obtained were different and this can be seen in Fig. 10.

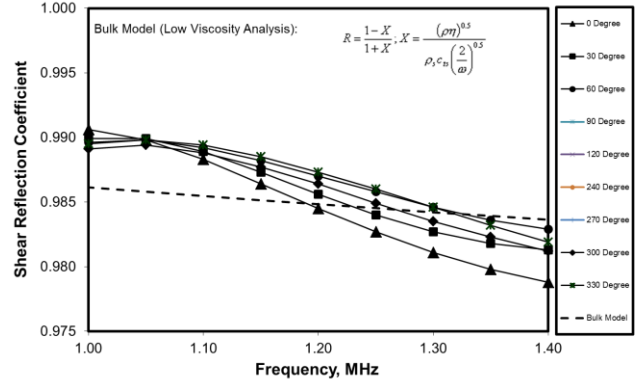


Figure 9 Experimental reflection coefficient spectra from 0^0 to 120^0 and 240^0 to 330^0 against the predicted spectra by the Bulk Model

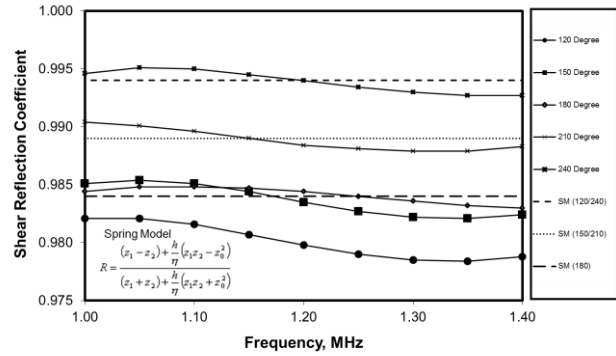


Figure 10 Experimental reflection coefficient spectra from 120^0 to 240^0 against the predicted spectra by the Spring Model

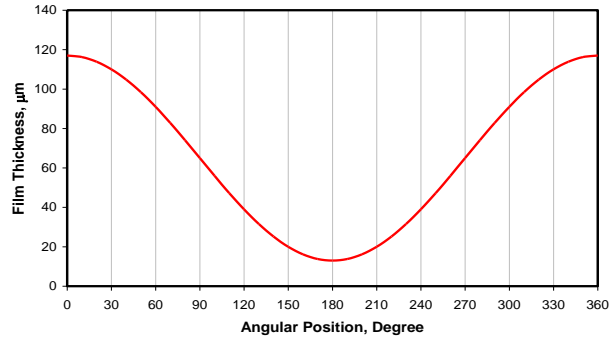


Figure 11 Film thickness profile determined from the eccentricity ratio

It was found that the internal lining of the bearing in this 90^0 to 180^0 region was slightly rough due to the minimum thickness that was established in this region. It was found that the surface had worn out more as compared to other areas. In this region, the thickness was found to be uneven and larger and this had caused the experimental reflection coefficient to be different.

C. Conversion To Viscosity

Reflection coefficient data in Fig. 7 were converted to viscosity by using the two models described earlier. The bulk model in (3) was used and the results obtained are shown in Fig. 12. The viscosity values by the bulk model agreed well in the regions between 0^0 to 60^0 and 270^0 to

360° regions where film thickness was thicker. In the other regions of thinner film layers, the viscosity values agree poorly.

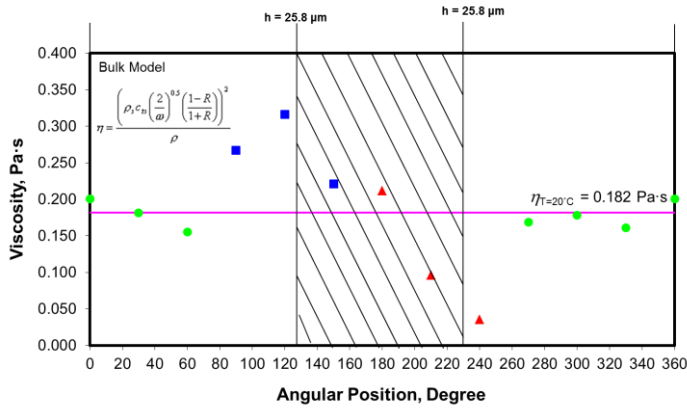


Figure 12 Viscosity values from the experimental reflection coefficient data determined by the bulk model

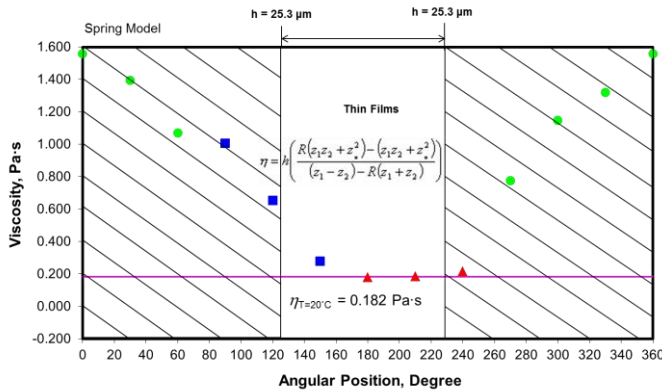


Figure 13 Viscosity values from the experimental reflection coefficient data determined by the spring model

The viscosity values computed by the spring model in Fig. 13 show a good agreement but only in the 180° to 240° region. The uneven surface on the internal lining of the bearing was suspected as the cause of the poor agreement in the region of 90° to 180°. The higher discrepancy of measured and predicted results by the spring model observed in the 180° to 240° region was as expected.

V. CONCLUSION

Work to map the viscosity profile around a journal bearing circumference has been described. A similar procedure to earlier work [4, 10] was carried out in order to get the shear reflection coefficient around the journal bearing circumference. The reflection coefficient profile that was observed became less dependent on frequency as the lubricant became thinner.

Where the bulk model was used, it appears that the viscosity measurements in thick films were poor especially in the region near the oil supply hole. In the case of the spring model, the viscosity results in thin films in the converging section were found to be within reasonable agreement and consistent. This is due to the shear stiffness value for thinner layer which is much higher than that of the thicker layer.

This study serves as a preliminary for further work on viscosity measurement to be conducted in a rotating journal bearing.

REFERENCES

- [1] M.S. Greenwood and J.A. Bamberger, "Measurement of viscosity and shear wave velocity of a liquid or slurry for on-line process control." *Ultrasonics*, 2002, 39(9), 623-630.
- [2] V.V. Shah and K. Balasubramaniam, "Measuring Newtonian viscosity from the phase of reflected ultrasonic shear wave." *Ultrasonics*, 2000, 38(1), 921-927.
- [3] S. Kasolang and R.S. Dwyer-Joyce, "Viscosity measurement in thin films using ultrasonic reflection." *Proc. IMechE*, 2008, Vol. 222 Part J: J. Engineering Tribology.
- [4] S. Kasolang and R.S. Dwyer-Joyce, "Viscosity measurement in bulk and thin Fluid." 34th Leeds-Lyon Symposium on Tribology, September 4-7 INSA de Lyon, France, (2007)
- [5] J. Blitz, "Fundamentals of ultrasonics, Plenum Press, New York. 1967.
- [6] G. Harrison and A.J. Barlow, "Dynamic viscosity measurement." *Methods of Exp. Physics*, 1981, 19, 137-178.
- [7] R. S. Dwyer Joyce, B. W. Drinkwater and C. J. Donohoe, "The measurement of lubricant-film thickness using ultrasound." *Royal Society*, 459, 957-976 (2003).
- [8] H. G. Tattersall, "The ultrasonic pulse-echo technique as applied to adhesion testing." *Applied Physics*, 1973, 6, 891-832.
- [9] G. Lian and M. Li, "Ultrasonic evaluation for the slip interface between two solids." *Shengxue Xuebao/Acta Acustica*, 2005, 30(1), 21-25.
- [10] S. Kasolang and R.S. Dwyer Joyce, "Observation of Film Thickness Profile and Cavitation Around a Journal Bearing Circumference." *Tribology Transaction*, 2008, 51: 231-245.